

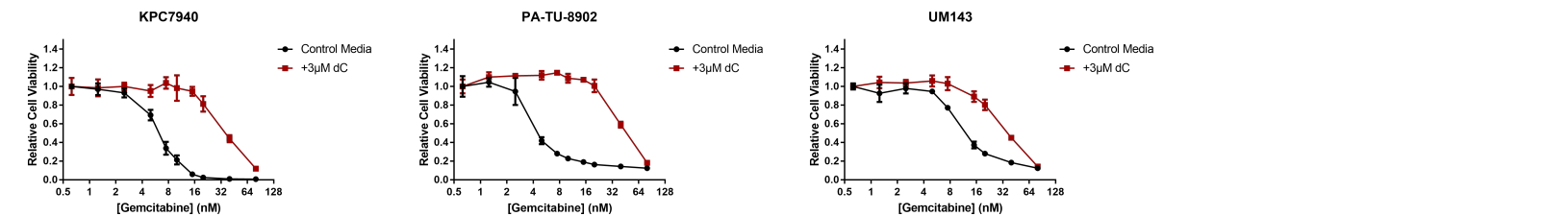
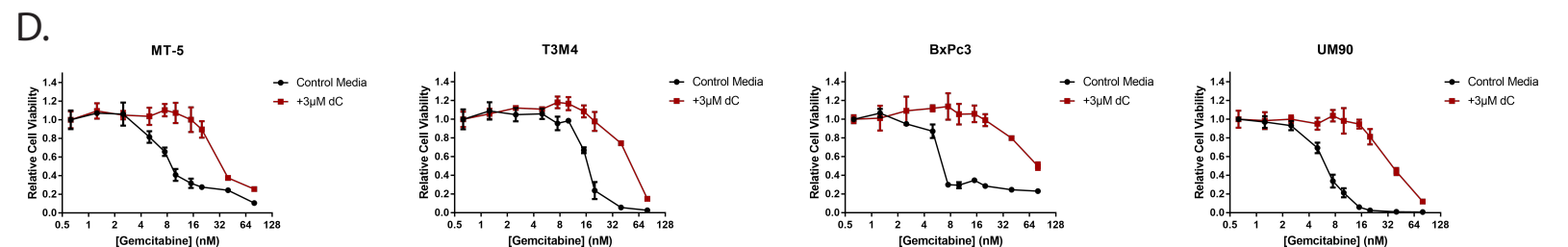
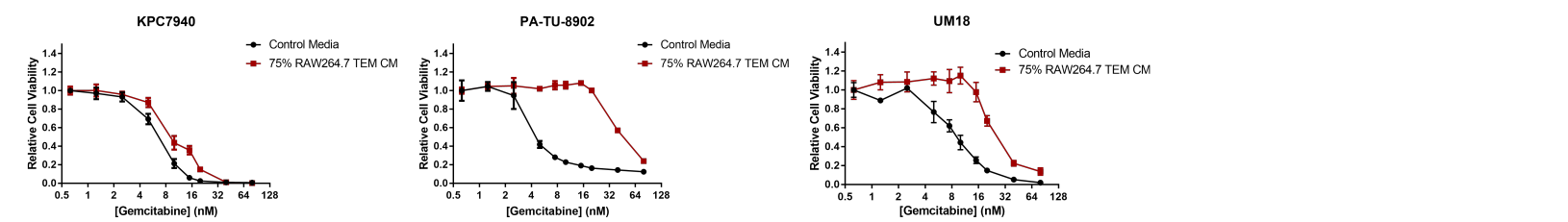
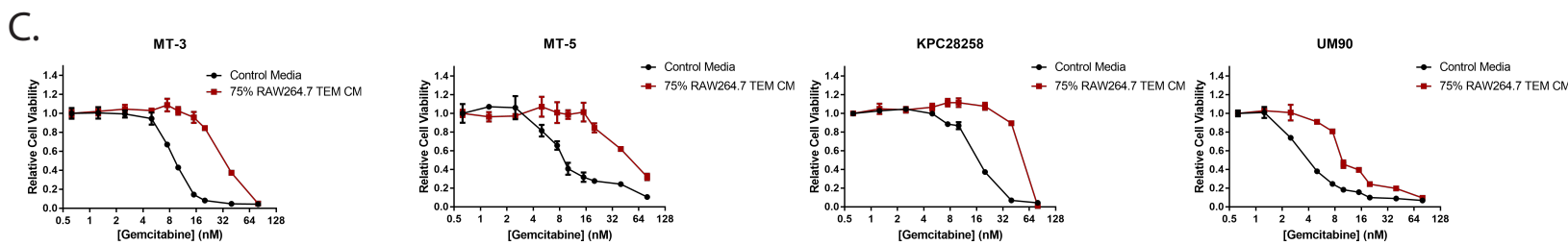
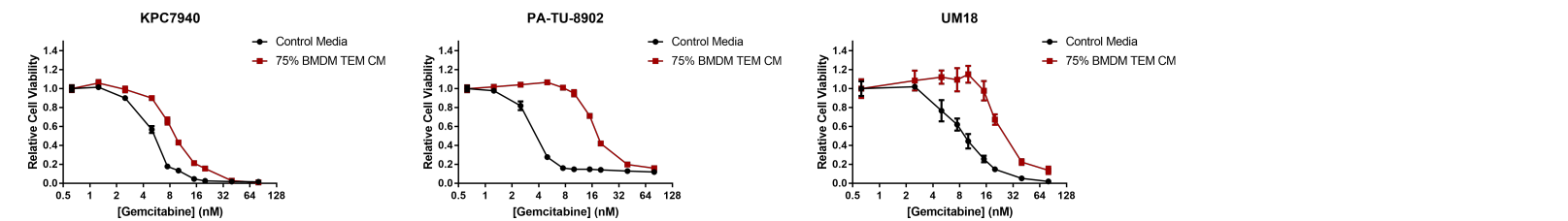
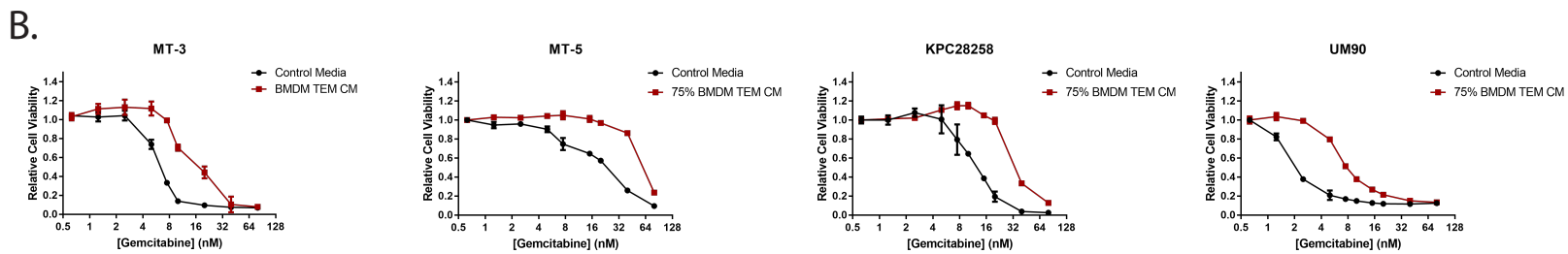
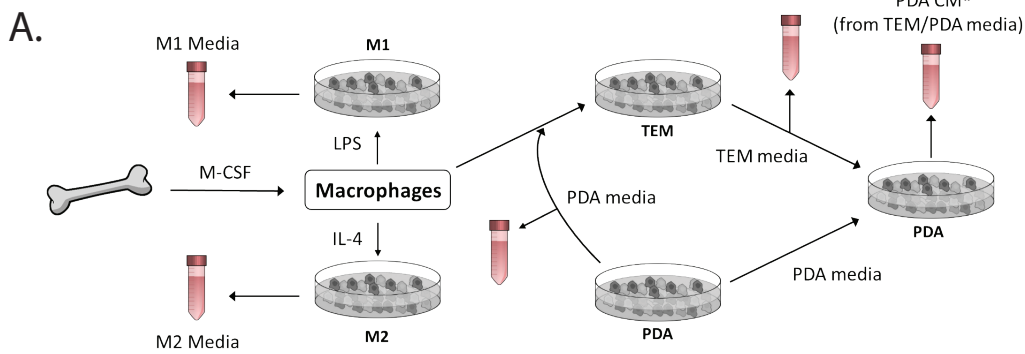
Supplemental Information

Macrophage-Released Pyrimidines

Inhibit Gemcitabine Therapy

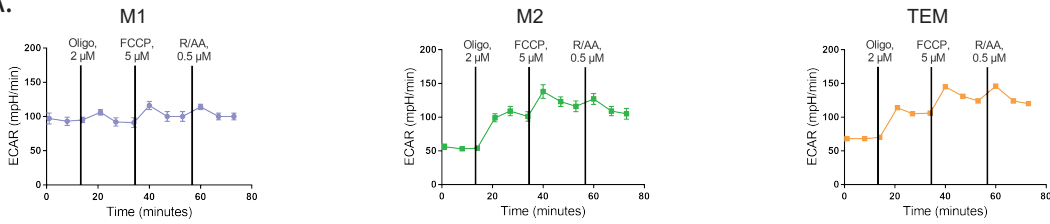
in Pancreatic Cancer

Christopher J. Halbrook, Corbin Pontious, Ilya Kovalenko, Laura Lapienyte, Stephan Dreyer, Ho-Joon Lee, Galloway Thurston, Yaqing Zhang, Jenny Lazarus, Peter Sajjakulnukit, Hanna S. Hong, Daniel M. Kremer, Barbara S. Nelson, Samantha Kemp, Li Zhang, David Chang, Andrew Biankin, Jiaqi Shi, Timothy L. Frankel, Howard C. Crawford, Jennifer P. Morton, Marina Pasca di Magliano, and Costas A. Lyssiotis

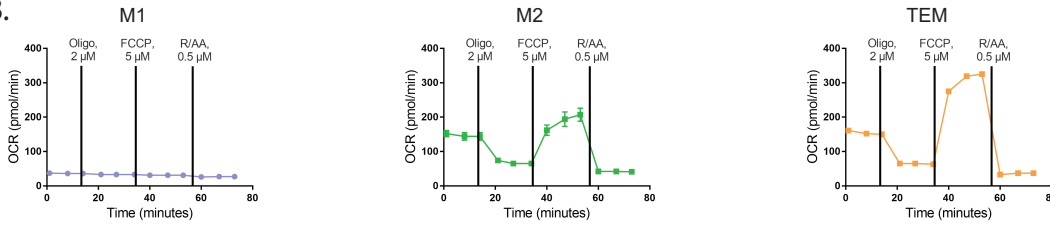


Supplemental Figure 1, Related to Figure 1: *TEMs provide gemcitabine resistance across a panel of PDA cell lines*. **S1a**. Schematic of bone marrow derived macrophage (BMDM) differentiation and polarization paradigm. **S1b**. Representative relative viability gemcitabine dose response curves in the presence of 75% BMDM TEM conditioned media vs. control media. Error bars are s.d., each point a technical replicate (n=3). IC₅₀ values derived from these dose response curves are plotted in **Fig. 1e**. **S1c**. Representative relative viability gemcitabine dose response curves in the presence of 75% RAW 264.7 (RAW) TEM conditioned media vs. control media. Error bars are s.d., each point a technical replicate (n=3). IC₅₀ values derived from these dose response curves are plotted in **Fig. 1f**. **S1d**. Representative relative viability gemcitabine dose response curves in the presence of complete DMEM supplemented with 3μM deoxycytidine (dC) vs. normal complete DMEM. Error bars are mean ± s.d., each point a technical replicate (n=3). IC₅₀ values derived from these dose response curves were plotted in **Fig. 1m**.

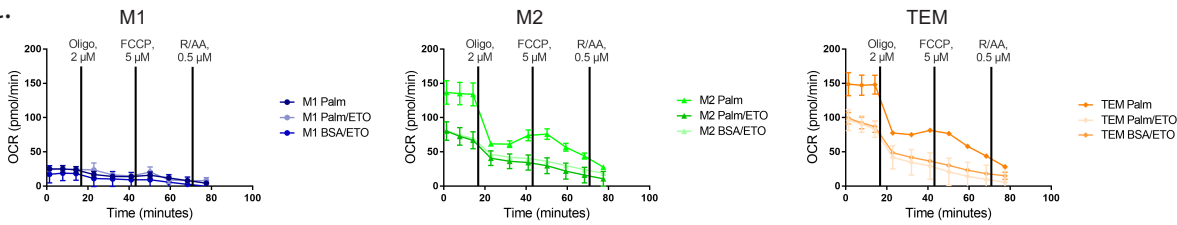
A.



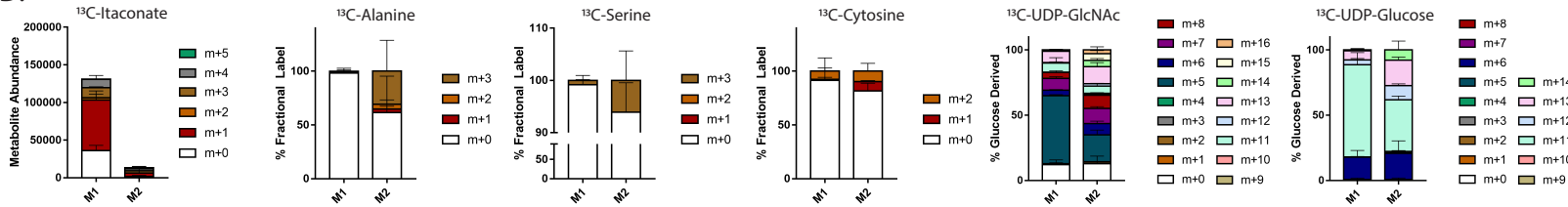
B.



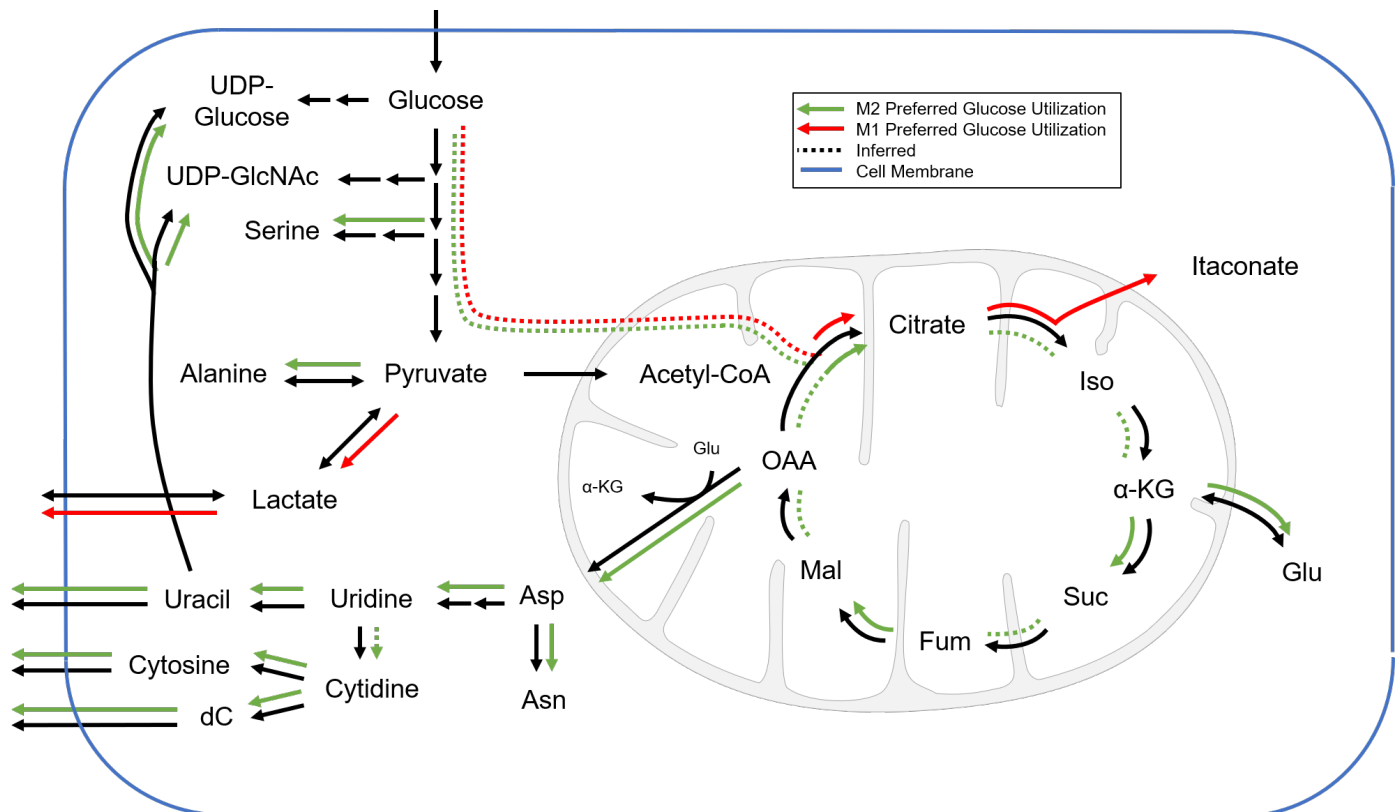
C.



D.



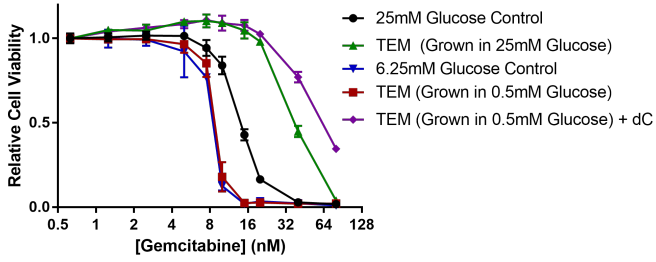
E.



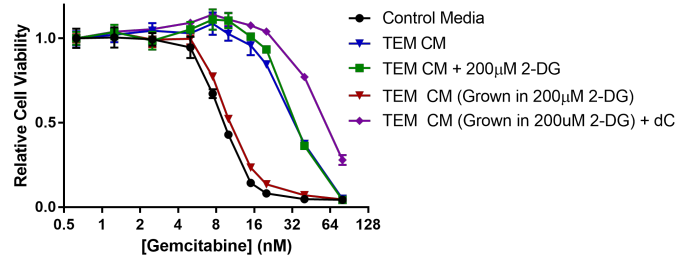
Supplemental Figure 2, Related to Figure 2: *Metabolic properties of macrophage subtypes*.

S2a,b. Seahorse mitostress assay of TEM, M1 and M2 macrophages measuring **S2a.** ECAR and **S2b.** OCR under standard conditions. Basal ECAR and OCR data were plotted in the bar graphs in **Fig.2b,c** and the Energy Profile in **Fig.2d**. Error bars are s.d., each point a technical replicate (n=5). **S2c.** Seahorse mitostress assay of TEM, M1 and M2 macrophages in fatty acid oxidation assay media supplemented with either Palmitate (Palm) as carbon source, Palm + fatty acid oxidation (FAO) inhibitor etomoxir (ETO), or bovine serum albumin (BSA) + ETO. Basal exogenous FAO data were plotted in the bar graph in **Fig.2e**. Error bars are s.d., each point a technical replicate (n=5). **S2d.** Isotopologue abundance of itaconate and fractional isotopologue labeling from ^{13}C -glucose in M1 vs. M2 macrophages. Error bars represent s.d. of biological replicates (n=3). **S2e.** Schematic summary of metabolic tracing data from uniformly labeled ^{13}C -glucose in M1 vs. M2 macrophages. Black lines represent canonical glucose metabolism pathways. The red arrows represent metabolic pathway activity inferred from the tracing data in which M1 metabolic activity is greater than that of M2s; green arrows are used for metabolic pathways in which activity in M2s are dominant over that in M1s. The dashed lines indicate inferred pathway directionality based on labeling patterns. Acetyl-CoA, Acetyl coenzyme A; α -KG, alpha ketoglutarate; Asn, Asparagine; Asp, Aspartate; dC, deoxycytidine; Fum, Fumarate; Glu, Glutamate; Iso, isocitrate; Mal, Malate; OAA, Oxaloacetate; Suc, Succinate; UDP-GlcNAc, Uridine diphosphate N-acetyl-glucosamine; UDP-Glucose, Uridine diphosphate glucose.

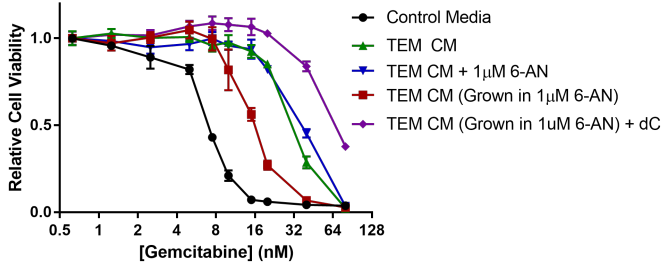
A.



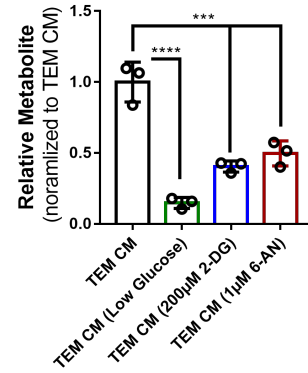
B.



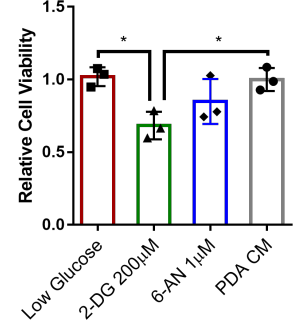
C.



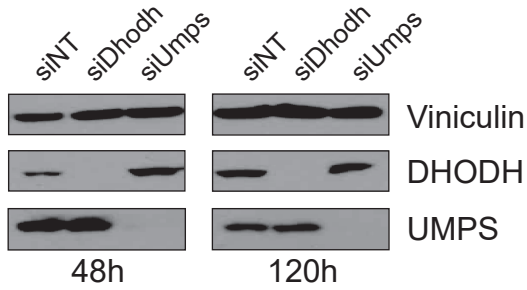
D.



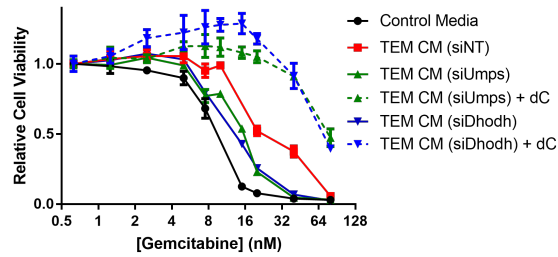
E.



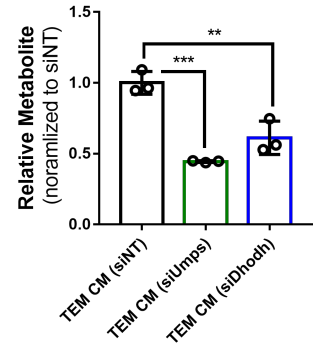
F.



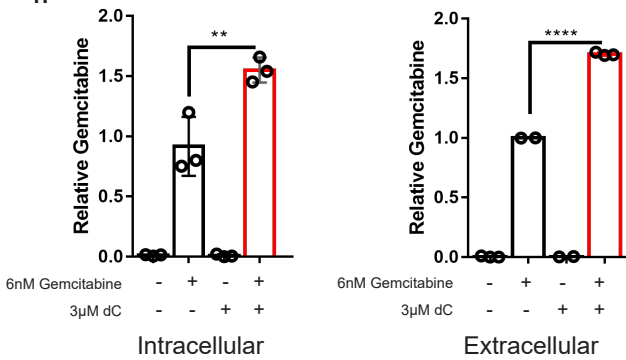
G.



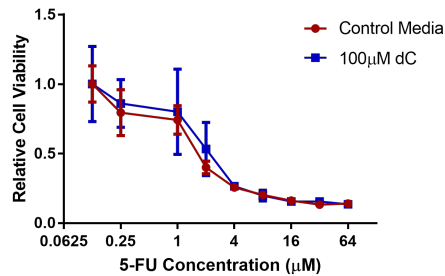
H.



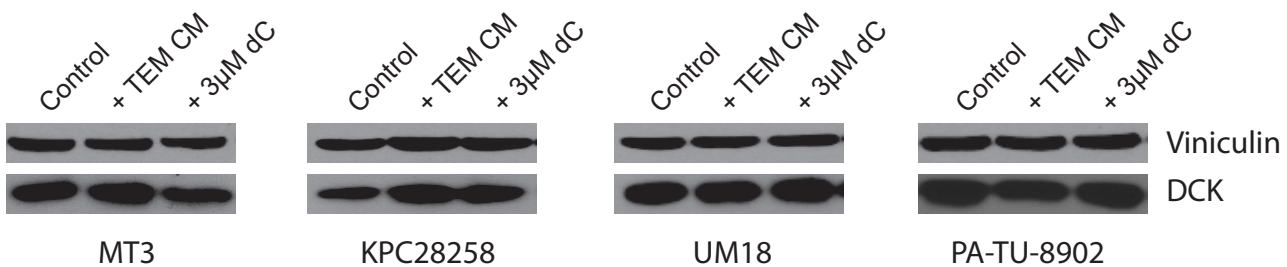
I.



J.



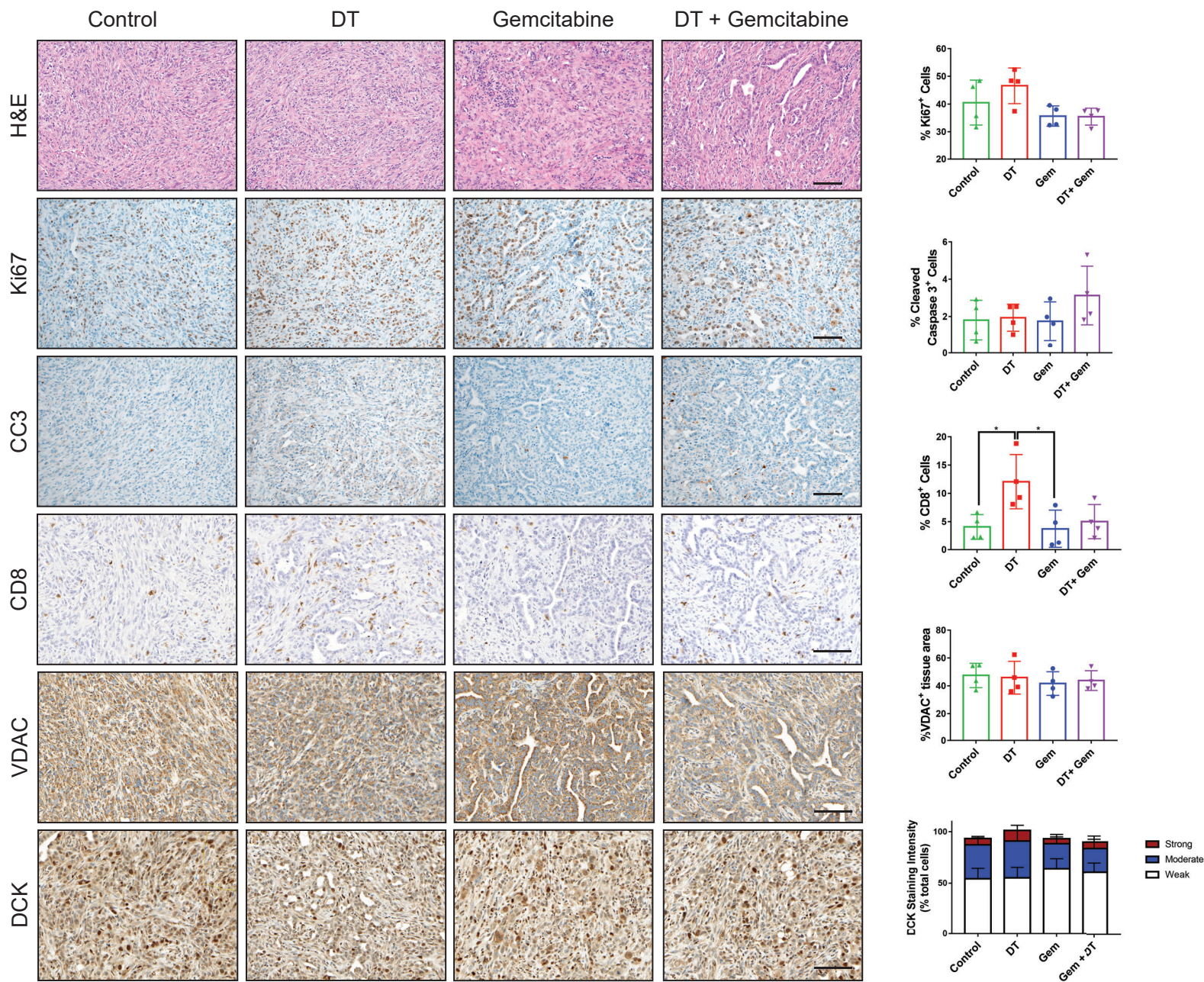
K.



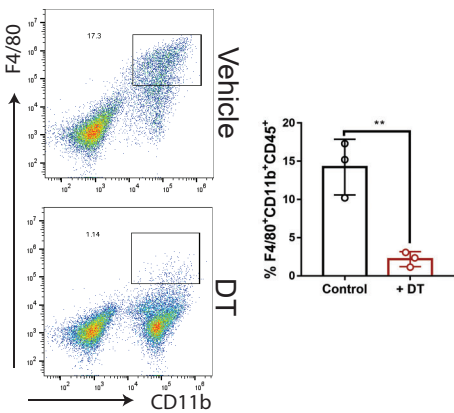
Supplemental Figure 3, Related to Figure 2,3: *Inhibition of de novo nucleotide biosynthesis blocks TEM mediated gemcitabine resistance*. **S3a**. Representative relative survival gemcitabine dose response curves for KPC-MT3 cells treated in normal glucose DMEM (25mM), 75% glucose restricted media (6.25mM), 75% conditioned media from TEMs grown in normal glucose DMEM, 75% conditioned media from TEMs grown in glucose restricted media, or 75% CM from TEMs grown in glucose restricted media + 3 μ M deoxycytidine (dC). Error bars are s.d., each point a technical replicate (n=3). IC₅₀ values derived from these dose response curves are plotted in **Fig. 2i**. **S3b**. Representative relative survival gemcitabine dose response curves for KPC-MT3 cells treated in normal DMEM, normal DMEM + 200 μ M 2-deoxyglucose (2-DG), 75% TEM conditioned media, 75% conditioned media from TEMs grown in 200 μ M 2-DG, or 75% conditioned media from TEMs grown in 200 μ M 2-DG + 3 μ M dC. Error bars are s.d., each point a technical replicate (n=3). IC₅₀ values derived from these dose response curves are plotted in **Fig. 2m**. **S3c**. Representative relative survival gemcitabine curves for KPC-MT3 cells treated in normal DMEM, normal DMEM + 1 μ M 6-aminonicotinamide (6-AN), 75% TEM conditioned media, 75% conditioned media from TEMs grown in 1 μ M 6-AN, or 75% conditioned media from TEMs grown in 1 μ M 6-AN + 3 μ M dC. Error bars are s.d., each point a technical replicate (n=3). IC₅₀ values derived from these dose response curves are plotted in **Fig. 2n**. **S3d**. Relative levels of dC present in normal TEM conditioned media, glucose deprived TEM conditioned media, TEM conditioned media grown in 200 μ M 2-DG, or TEM conditioned media grown in 1 μ M 6-AN (n=3), as determined by LC/MS analysis, normalized to normal TEM media. **S3e**. Relative viability of TEMs in PDA conditioned media alone, PDA conditioned media + 200 μ M 2-DG, or PDA conditioned media + 1 μ M 6-AN. Error bars are s.d., each point a technical replicate (n=3). **S3f**. Western blot analysis of gene knockdown of RAW 246.7 TEMs transfected with either nontarget siRNA, or siRNAs targeted to *Dhodh* or *Umps*. **S3g**. Representative relative survival gemcitabine dose response curves for KPC-MT3 cells treated in normal DMEM, or 75% conditioned media from TEMs transfected with siRNA targeting *Dhodh*, *Umps*, or

nontargeting (NT) siRNA, or conditioned media from TEMs transfected with siRNA targeting *Dhodh*, *Umps* + 3 μ M dC. Error bars are s.d., each point a technical replicate (n=3). IC₅₀ values derived from these dose response curves are plotted in **Fig. 2o. S3h**. Relative levels of dC present in siNT TEM conditioned media, siUmps TEM conditioned media, or siDhodh TEM conditioned media (n=3), as determined by LC/MS analysis, normalized to siNT TEM conditioned media. **S3i**. Relative intra and extracellular abundance of gemcitabine in KPC-28258 cells or extracellular media, respectively, after 16 hours of treatment with 6nM gemcitabine in the presence or absence of 3 μ M dC, as measured by LC-MS/MS. Error bars represent s.d., samples were prepared from individual plates (n=3). **S3j**. Representative relative viability dose response curve of MT3-KPC cells treated with 5-FU in the presence of 100 μ M dC versus control media. Error bars represent s.d., each point represents a technical replicate (n=3). **S3k**. Western blot analysis of DCK expression in KPC-MT3, KPC 28258, UM18, and PA-TU-8902 PDA cells in normal control media, treated with TEM CM for 24 hours, or treated with 3 μ M dC for 24 hours. Vinculin serves as a loading control. Significance was calculated by one-way ANOVA with Tukey post hoc test, ** $P \leq 0.01$; **** $P \leq 0.0001$.

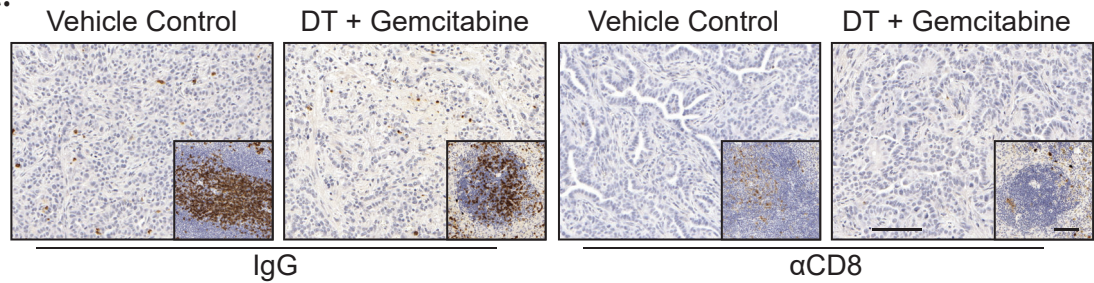
A.



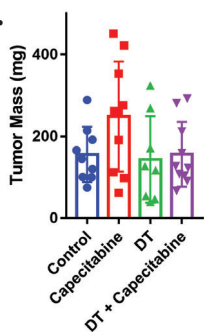
B.



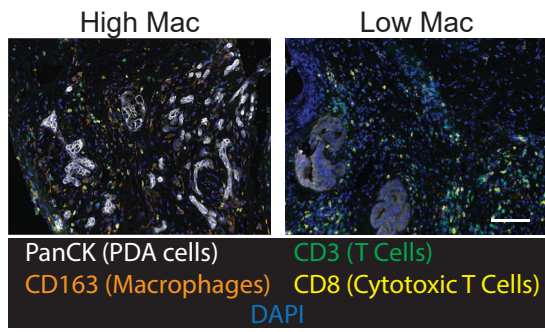
C.



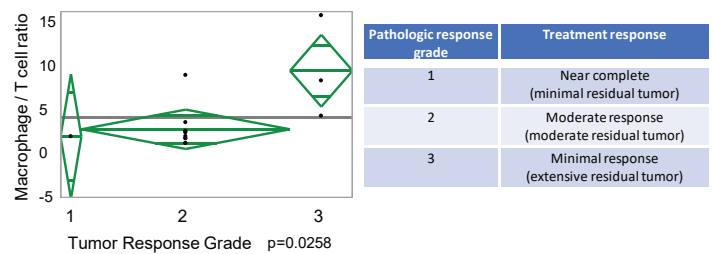
D.



E.



F.



Supplemental Figure 4, Related to Figure 4: *Murine and human data for chemotherapy-treated pancreatic tumors*. **S4a**. Histology and quantification of KPC-MT3 tumors from vehicle-, gemcitabine-, diphtheria toxin (DT)-, or gemcitabine + DT-treated Cd11b-DTR mice. CC3, cleaved caspase 3; H&E, Hematoxylin and Eosin. **S4b**. Density plot and quantification from flow cytometry analysis of macrophages (CD45⁺Cd11b⁺F4/80⁺) present in tumor of vehicle or diphtheria toxin (DT) treated mice 24 hours post treatment. **S4c**. Representative immunostaining of CD8 cells present in tumors quantified in **Fig. 4f** (inset: representative staining of CD8 cells in the spleen of the same mouse). **S4d**. Mass of KPC-MT3 tumors at endpoint from vehicle- (n=9), capecitabine- (n=10), DT- (n=8), or DT + capecitabine-treated (n=10) mice. Error bars represent s.d. **S4e**. Representative multiplex-immunofluorescence images of high vs. low macrophage containing neoadjuvant gemcitabine treated patient tumors. **S4f**. Correlation of pathological response, graded using the College of American Pathologists (CAP) tumor regression grading system, to the ratio of macrophages to T cells in neoadjuvant gemcitabine treated patient tumors (n=12). Scale bars = 100µm.

Species	Concentration (μM)	SD
Thymine	3.56	0.85
Thymidine	4.60	1.97
Uridine	17.25	5.37
Deoxyuridine	2.62	0.63
Cytosine	1.65	1.33
Cytidine	2.71	0.94
Deoxycytidine	3.16	0.95

Supplemental Table 1, Related to Figure 1: Calculated abundance of pyrimidines in TEM conditioned media, determined via LC-MS/MS from 3 separate TEM preparations. SD = standard deviation.

	Total	Expected	Hits	Raw p	LOG(p)	Holm adjust	FDR	Impact
Purine metabolism	68	5.3747	18	1.74E-06	13.26	0.00014297	0.00014297	0.34839
Arginine and proline metabolism	44	3.4778	13	1.52E-05	11.095	0.0012301	0.00062266	0.47887
Pyrimidine metabolism	41	3.2406	12	3.70E-05	10.204	0.0029623	0.00090521	0.34699
Aminoacyl-tRNA biosynthesis	69	5.4538	16	4.42E-05	10.028	0.0034884	0.00090521	0
Alanine, aspartate and glutamate metabolism	24	1.897	8	0.00029952	8.1133	0.023363	0.0049122	0.81118
Vitamin B6 metabolism	9	0.71136	4	0.0034174	5.6789	0.26314	0.046705	0.41176
beta-Alanine metabolism	17	1.3437	5	0.0080792	4.8185	0.61402	0.087446	0.44444
Glycine, serine and threonine metabolism	31	2.4502	7	0.0085313	4.764	0.63985	0.087446	0.39196
Glutathione metabolism	26	2.055	6	0.013245	4.3241	0.98013	0.12068	0.08683
Nitrogen metabolism	9	0.71136	3	0.028398	3.5614	1	0.23286	0
Phenylalanine, tyrosine and tryptophan biosynthesis	4	0.31616	2	0.033434	3.3982	1	0.24923	0.5
Glyoxylate and dicarboxylate metabolism	18	1.4227	4	0.047618	3.0445	1	0.28903	0.51612
Valine, leucine and isoleucine biosynthesis	11	0.86944	3	0.049665	3.0024	1	0.28903	0.99999
Biotin metabolism	5	0.3952	2	0.052872	2.9399	1	0.28903	0.4
D-Glutamine and D-glutamate metabolism	5	0.3952	2	0.052872	2.9399	1	0.28903	1
Amino sugar and nucleotide sugar metabolism	37	2.9245	6	0.065696	2.7227	1	0.32204	0.18595
Citrate cycle (TCA cycle)	20	1.5808	4	0.066765	2.7066	1	0.32204	0.24707
Histidine metabolism	15	1.1856	3	0.10889	2.2174	1	0.46995	0
Pantothenate and CoA biosynthesis	15	1.1856	3	0.10889	2.2174	1	0.46995	0
Taurine and hypotaurine metabolism	8	0.63232	2	0.12673	2.0657	1	0.5196	0.71428
Glycolysis or Gluconeogenesis	26	2.055	4	0.14371	1.94	1	0.53563	0.00653
Galactose metabolism	26	2.055	4	0.14371	1.94	1	0.53563	0.21695
Cysteine and methionine metabolism	27	2.1341	4	0.15898	1.839	1	0.5668	0.17491
Glycerophospholipid metabolism	30	2.3712	4	0.20804	1.57	1	0.67432	0.15278
Riboflavin metabolism	11	0.86944	2	0.21381	1.5427	1	0.67432	0

Phenylalanine metabolism	11	0.86944	2	0.21381	1.5427	1	0.67432	0.64815
Nicotinate and nicotinamide metabolism	13	1.0275	2	0.27449	1.2928	1	0.82256	0.20833
Lysine biosynthesis	4	0.31616	1	0.28087	1.2698	1	0.82256	0
Pentose and glucuronate interconversions	16	1.2646	2	0.3648	1.0084	1	1	0.2
Cyanoamino acid metabolism	6	0.47424	1	0.3904	0.9406	1	1	0
Tryptophan metabolism	40	3.1616	4	0.39058	0.94011	1	1	0.37356
Starch and sucrose metabolism	19	1.5018	2	0.45065	0.79705	1	1	0.31549
Ascorbate and aldarate metabolism	9	0.71136	1	0.52443	0.64544	1	1	0
Methane metabolism	9	0.71136	1	0.52443	0.64544	1	1	0
Butanoate metabolism	22	1.7389	2	0.52969	0.63547	1	1	0.02899
Lysine degradation	23	1.8179	2	0.55429	0.59007	1	1	0
Pyruvate metabolism	23	1.8179	2	0.55429	0.59007	1	1	0.01375
Valine, leucine and isoleucine degradation	38	3.0035	3	0.5898	0.52797	1	1	0
Porphyrin and chlorophyll metabolism	27	2.1341	2	0.64351	0.44081	1	1	0
Selenoamino acid metabolism	15	1.1856	1	0.71105	0.34102	1	1	0
Glycerolipid metabolism	18	1.4227	1	0.77495	0.25495	1	1	0.0256
Pentose phosphate pathway	19	1.5018	1	0.79297	0.23197	1	1	0.03078
Propanoate metabolism	20	1.5808	1	0.80956	0.21127	1	1	0
Fructose and mannose metabolism	21	1.6598	1	0.82482	0.19258	1	1	0.03142
Primary bile acid biosynthesis	46	3.6359	2	0.8919	0.11441	1	1	0.05952
Inositol phosphate metabolism	28	2.2131	1	0.90258	0.1025	1	1	0
Biosynthesis of unsaturated fatty acids	42	3.3197	1	0.97015	0.030308	1	1	0
Fatty acid biosynthesis	43	3.3987	1	0.97258	0.027804	1	1	0

Supplemental Table 2, Related to Figure 2: Metaboanalyst pathway enrichment analysis.

Compound	Primary Transporter	Activating Kinase	Inhibited by 3μM dC
Gemcitabine	CNT>ENT	dCK	8 fold
5-aza-dC	ENT~CNT	dCK	4 fold
5-aza-C	ENT~CNT	UCK	0
Trifluorothymidine	CNT>ENT	TK	0
Fialuridine	ENT~CNT	TK	0
5-FU	OAT2	TYMS	0
dC	ENT>CNT	dCK	N/A

Supplemental Table 3, Related to Figure 3: Table of deoxycytidine and anti-pyrimidine metabolites, their reported transporters, activating kinases, and inhibition by deoxycytidine treatment. 5-aza-dC, 5-aza-dexoycytidine; 5-aza-C, 5-aza-cytidine; 5-FU, 5-fluorouracil; CNT, concentrative nucleoside transporter; dCK = deoxycytidine kinase; ENT, equilibrative nucleoside transporter; OAT2, organic anion transporter 2; TK, thymidine kinase; TYMS, thymidylate synthetase; UCK, uridine-cytidine kinase.

Supplemental Table 4, Related to Figure 4: De-identified patient data presented in Fig. 4i,j and detailed in STAR Methods.